A Numerical Method for the Design and Analysis of Counter-Rotating Propellers

S. C. Playle,* K. D. Korkan,† and E. von Lavante‡
Texas A&M University, College Station, Texas

A numerical method has been developed using the techniques of Lock and Theodorsen as described by Davidson to design and analyze counter-rotating propellers. The design method develops the optimum propeller geometry by calculating the planform and twist distribution for each propeller disk through the use of specific inputs of engine shaft horsepower, diameter, and disk spacing. The analysis method calculates the performance of a given counter-rotating propeller system at any flight condition. Using the NACA four-digit airfoil family, the performance of a counter-rotating propeller design for a given flight condition was investigated in the design and analysis mode.

Nomenclature

A = propeller disk area
B = interference angle
b_k = Betz's coefficient
c = chord
C_D = drag coefficient
C_L = lift coefficient
C_P = power coefficient
C_Q = torque coefficient
C_T = thrust coefficient
D = diameter
J = advance ratio
$K(x)$ = circulation
ℓ = inverse lift-to-drag ratio
M = Mach number
n = revolutions per second
SHP = shaft horsepower
p = ambient pressure, constant of calculation
Q = torque
q = freestream dynamic pressure, constant of calculation
R = radius
r = radial distance, constant of calculation
s = constant of calculation
T = thrust
u = axial interference velocity
V = freestream velocity
v = radial interference velocity
W = resultant velocity
w = rearward helical displacement velocity
X_0 = tip loss factor
x = percent radial location
α = angle of attack
β = blade twist angle
γ, δ_{AF} = angles defined in Figs. 1 and 2
δ_{RB}, δ_{AB} = angles defined in Fig. 2
η = propeller efficiency
ρ = ambient air density
σ = solidity
ϕ = resultant velocity angle
ϕ_0 = advance angle
Ω = rotational velocity
ω = downwash velocity

Subscripts

B = back propeller disk
F = front propeller disk

Presented as Paper 84-1205 at the AIAA/SAE/ASME 20th Joint Propulsion Conference, Cincinnati, OH, June 11-13, 1984; received April 15, 1985; revision received Sept. 4, 1985.

*Graduate Research Assistant, Aerospace Engineering Department. Student Member AIAA.

†Associate Professor, Aerospace Engineering Department. Associate Fellow AIAA.

‡Assistant Professor, Aerospace Engineering Department. Member AIAA.

I. Introduction

THERE has been renewed interest in finding a more efficient replacement for current aircraft propulsion systems, with one such approach utilizing a counter-rotating propeller configuration. An initial theory regarding the mechanics of counter-rotating propellers was developed by Lock[1] in 1941. Since then, many investigations into the advantages of counter-rotating propellers have been conducted. For example, Biermann and Gray[2] conducted full scale wind tunnel tests on counter-rotating propellers in both tractor and pusher configurations. It was found that an 8 to 16% increase in propeller efficiency could be gained depending upon installation position. In a later test, Biermann and Hartman[3] found that the performance of counter-rotating propellers was significantly improved at lower advance ratios. McHugh and Pepper[4] have shown that the counter-rotating propeller configuration is highly receptive to the use of aerodynamically improved airfoil designs. Other investigations into the performance of counter-rotating propellers conducted by Gray[5] have indicated that the overall efficiency of a counter-rotating propeller is not seriously affected by changes in rotational speed or small changes in blade angle of the aft propeller disk. These changes did, however, have a moderate effect when the propeller was operated at peak efficiency. In an experimental study, Miller[6] found that the vibration of counter-rotating propellers caused by mutual blade passage or by blade passage through the wake of a wing was not significant. Bartlett[7] has shown that locking or windmilling one of the propeller components of a counter-rotating configuration has a detrimental effect on total propeller efficiency. For example, a counter-rotating propeller with one propeller disk disabled results in a total propeller efficiency that is lower than the individual efficiency of the rotating propeller.

This brief literature survey has indicated that counter-rotating propellers exhibit many advantages over single-rotation propellers such as higher peak efficiency, better off-design performance, and a reduced total torque of the system.

The increase in peak efficiency and improved off-design performance of counter-rotating systems allow for smaller propulsion units to be installed on the aircraft. The disadvantages of counter-rotating propeller configurations include gearbox complexity and an increased vibrational state caused by the periodic blade passage. Research conducted by Strack et. al.[8] has shown that with current improvements of present day technology, lightweight and reliable counter-rotating propeller gearboxes can be built. Thus, it is evident that counter-rotating propellers can indeed offer a more efficient means of propulsion.

The work described previously has been limited in the analysis of counter-rotating propeller configurations. Therefore, it is necessary to develop a consistent methodology to obtain a design approach as well as detailed analyses of counter-rotating propeller systems. In the present study, existing theoretical models for the design and analysis of counter-rotating propellers were investigated and compared to determine a method that could be developed for use as a design and analysis method.

II. Selection of Design Method

The majority of the work described in the previous section was conducted with existing single-rotation propeller blades in a counter-rotating configuration. Therefore, a requirement to develop a theoretical means by which counter-rotating propellers could be designed and analyzed was initially investigated. Three previously developed theoretical models for the design of counter-rotating propellers were considered and examined for feasibility of further development.

The first method, developed by Ginzel,[9] makes no presumption about the distribution of spanwise circulation across the blade. It is restricted to the use of aerodynamics that result from propellers, which were built in accordance with the structural constraints that existed at the time the theory was developed. This structural restriction was applied in 1943 and is not pertinent with respect to the current state of technology. For example, with the advent of composite materials and high strength alloy metals, the structural assumptions that Ginzel based his method on are no longer valid.

Other methods for the design of counter-rotating propellers include the SBAC method[10] and a theoretical model developed at United Technologies Research Center (UTRC).[11] The SBAC method is computationally very cumbersome as it is a design-by-analysis method and requires data interpolation and cross referencing, and the UTRC method requires extensive computer time and memory.

In another method, Naiman[12] uses a modified strip theory in which approximations for the interference relations from the front and aft propeller disks are assumed such that the interference calculations are functions of each propeller disk independently. Naiman uses sectional aerodynamic characteristics as a basis for his derivations, and hence allows the use of various families of airfoils and different structural constraints. Sectional circulation to determine the interference relations is also utilized by Naiman, and therefore the method is adaptable to changing technology.

Another counter-rotating propeller calculation method investigated was that of Lock[1] and Theodorsen[13,14] as described by Davidson.[15] This method uses an interpolation scheme between both propeller disks for the interference of one disk upon the other, and requires the use of the circulation of the entire configuration as an input for calculation of the interference relations. Similar to Naiman's method, Davidson's approach is easily expanded to off-design analysis.

Since Ginzel's method was considered unacceptable, as were the SBAC and UTRC methods for ease of use and applicability to design, the methods of Naiman and Davidson were chosen for further development and investigation. The results of computer-generated designs for these two theoretical models were compared to determine which model was superior for reasons of accuracy, computational efficiency, and further development. The results of the comparison of the two methods by Playle[16] have shown that the Lock and Theodorsen method, given by Davidson, was more accurate. Davidson's approach yielded realistic designs of counter-rotating propeller configurations in terms of planform and performance values and was adaptable to further development. In addition, inclusion of drag and compressibility shown in this work were the most useful modifications using this theoretical approach. Davidson's method was also found to be adaptable to include off-design analysis, disk spacing, blade sweep, and different angular velocities on each propeller disk.[16]

III. Theoretical Design Development

The main advantage of counter-rotating propellers stems from the swirl velocity losses of the front propeller disk being recovered by the aft propeller disk. The front disk imparts a tangential velocity to the air as it passes through the front propeller disk plane. This swirl velocity acts as an additional angular velocity for the aft disk, without the power plant having to drive the aft disk at a higher angular velocity. Figures 1 and 2 show the velocity diagrams for the front and aft disk, respectively. It may be noted that a tangential interference velocity is recognized by the front disk, but is typically an order-of-magnitude smaller than other interference velocities and therefore neglected, resulting in a first-order theory for the design and analysis of counter-rotating propellers.

Airfoil data, such as lift, drag, and angle of attack are specified for each radial location along the propeller blade. This is done through the use of airfoil data banks, utilizing either tabulated data or empirical formulations that yield airfoil lift and drag as functions of angle of attack and Mach number.[17] The airfoil data used in the calculations during the design process was selected to maximize the lift-to-drag ratio of the airfoil used at each radial location along the blade. In regions near the hub, where the propeller blade quickly transitions from an airfoil to a right circular cylinder, a different approach has been taken. To accommodate this transition, the chord length is linearly interpolated from that calculated to a structurally feasible cylinder at the hub. The design procedure involves calculations, which include division by the lift coefficient, to determine chord length. Since the lift coefficient of a circular cylinder is zero, it may be noted in the development of the theoretical model that it is necessary to maintain a finite-lift coefficient to insure arriving at positive values of the blade chord.

Once the airfoil data have been specified, a comparison scheme is initiated whereby the power input to the propeller and the power absorbed by the propeller are matched. This iteration scheme begins with an assumed value for the propeller efficiency, which need not be accurate since η will be changed by the iteration process. From the assumed propeller efficiency Betz's coefficient is calculated, which is the parameter through which the iteration process is conducted. Davidson has derived Betz's coefficient using calculus of optimization as:

$$b_k = 4(1-\eta) \tag{1}$$

Calculation of the rearward helical displacement velocity[14] may be accomplished by the expression

$$w^2 = 2p/\rho[(1+0.2M_\infty^2)^{3.5} - 1] \tag{2}$$

Using the experimental values of circulation by Theodorsen[13] as a function of r/R and $(V+w)/nD$, the circulation $K(x)$ can be found for each radial location as noted in Fig. 3.

The present method for designing and analyzing counter-rotating propeller configurations is two-dimensional by virtue of the strip-analysis approach. However, the propeller is primarily a three-dimensional flow phenomena, and therefore a method to include the difference between two- and three-

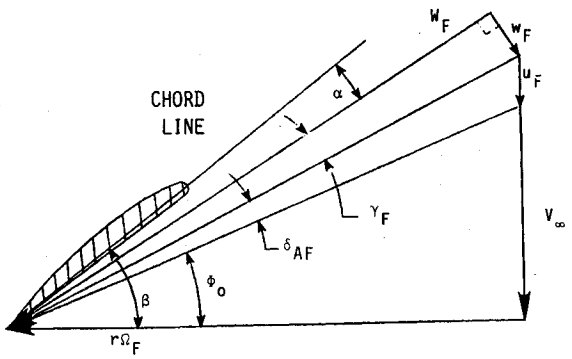

Fig. 1 Velocity diagram for front propeller disk.

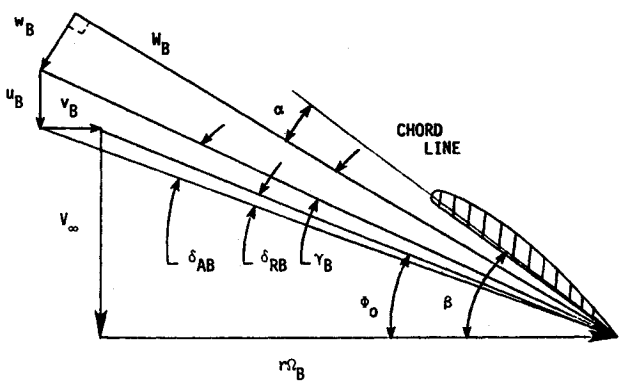

Fig. 2 Velocity diagram for back propeller disk.

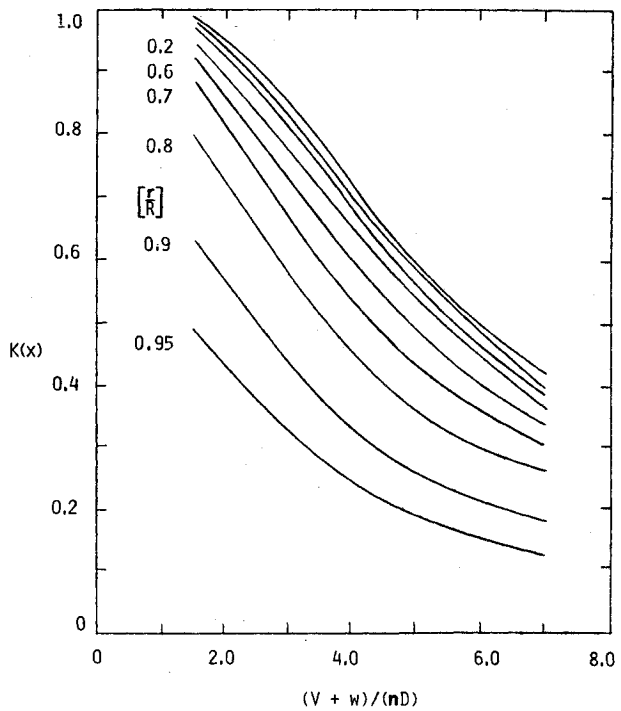

Fig. 3 Circulation function for dual-rotation propellers; four blades, front and back propeller disks (Ref. 13).

dimensional flow is required. Davidson derived a version of Lock's tip-loss factor[15] for specific application to counter-rotating propellers, which is a well behaved function that is different from a single-rotation propeller. A reformulation for Lock's tip-loss factor that includes drag has been derived[15,16] and takes the form

$$X_0 = qs/(2p - qrs) \tag{3}$$

where

$$p = \frac{\frac{1}{2}}{\cos\phi_0}\left(\sin\phi_0 + \frac{C_D}{C_L}\cos\phi_0\right)$$

$$q = \frac{1}{2\sin\phi_0}, \quad r = \cos^2\phi_0 - \sin^2\phi_0,$$

$$s = (J/\pi x)/[K(x)\sin\phi_0] \tag{4}$$

The solidity-lift coefficient for each radial location on each disk is then given by

$$\sigma C_L = \left[\frac{\frac{1}{2}}{b_k}\left(\sin\phi_0 + \frac{C_D}{C_L}\cos\phi_0\right)\cos\phi_0 - \frac{C_D}{C_L}\right] \div \left[\frac{1}{2\sin\phi_0}\left(\frac{1}{X_0} + \cos^2\phi_0 - \sin^2\phi_0\right)\right] \tag{5}$$

with the value of C_D/C_L arrived at through use of the airfoil data banks. Having calculated the solidity-lift coefficient, the differential power coefficients, which are measures of the power absorbed by each propeller disk, can be computed by

$$\frac{dC_p}{dx} = \frac{\pi^4}{4}(\sec^2\phi_0)x^4\sigma C_L\left(\sin\phi_0 + \frac{C_D}{C_L}\cos\phi_0\right) \tag{6}$$

Equation (6) is integrated to find the total power coefficient for the power absorbed by both the front and aft propeller disk. The power absorbed is compared to the power input to the propeller by the power plant, which is dictated by the available horsepower of the power plant specified in power coefficient form by

$$C_P = 550\,\mathrm{SHP}/\rho n^3 D^5 \tag{7}$$

If the two values of the power coefficient do not match within a given tolerance, Betz's coefficient is adjusted and the power absorbed is recalculated following the outlined procedure. The adjustment made to Betz's coefficient represents alterations in the planform of the propeller blade, and thus propeller blade loading. Should the power absorbed be lower or higher than the power input, Betz's coefficient is increased or decreased, respectively. The iteration process is continued until the power absorbed by the propeller is within a predetermined percentage of the power input to the propeller.

The condition of the power absorbed by the propeller being equal to the power input, defines the optimum propeller for the given flight conditions since the configuration was designed using the maximum lift-to-drag ratio for the chosen airfoil at each radial location. Also, since the form of Betz's coefficient has been determined through calculus of optimization and used as the iteration parameter, the resulting design is considered to be the optimum counter-rotating propeller for the input condition.

The physical geometry of the propeller is calculated once the solidity-lift coefficient radial distribution has been defined through the above iteration process. By iterating between the resultant interference velocities and the resultant total velocity, both the interference and total velocities can be found by the following expressions:

$$W_F = r\,\Omega_F \sec\phi_0 \cos(\phi_F - \phi_0) + u_F \sin\phi_F \tag{8}$$

$$W_B = r\,\Omega_B \sec\phi_0 \cos(\phi_F - \phi_0) + u_B \sin\phi_B + v_B \cos\phi_0 \tag{9}$$

$$u_F = X_0 \omega_{1B} \cos\phi_0 \tag{10}$$

$$u_B = X_0 \omega_{1F} \cos\phi_0 \tag{11}$$

$$v_B = 2X_0\omega_{1F}\sin\phi_0 \tag{12}$$

where

$$\omega_1 = \phi C_L W/4X_0\sin\phi_0 \tag{13}$$

The differential thrust and torque are functions of the resultant velocities and calculated by the following expressions:

$$\frac{dT}{dr} = \pi\rho r\sigma C_L W^2\left(\cos\phi_0 - \frac{C_D}{C_L}\sin\phi_0\right) \tag{14}$$

$$\frac{dQ}{dr} = \pi\rho r^2\sigma C_L W^2\left(\sin\phi_0 - \frac{C_D}{C_L}\cos\phi_0\right) \tag{15}$$

Integration of Eqs. (14) and (15) results in values of thrust and torque, hence the thrust coefficient, torque coefficient, and efficiency, i.e.,

$$C_T = \frac{T}{\rho n^2 D^4} \tag{16}$$

$$C_Q = \frac{Q}{\rho n^2 D^5} \tag{17}$$

$$C_P = 2\pi C_Q \tag{18}$$

$$\eta = C_T J/C_P \tag{19}$$

At this point, the radial values of the blade planform and twist distribution for each propeller disk can be calculated from

$$\text{Chord} = 2\pi r\sigma C_L/(\text{No. Blades})C_L \tag{20}$$

$$\beta = \phi_0 + B + \alpha \tag{21}$$

where

$$B_F = (\sigma C_{L_F}/4X_0\sin\phi_0)(1 + X_0\cos^2\phi_0) \tag{22}$$

$$B_B = (\sigma C_{L_B}/4X_0\sin\phi_0)(1 + X_0\cos^2\phi_0 - 2\sin^2\phi_0) \tag{23}$$

It is noted that the values for angle of attack were selected through the iteration process. In the present method, which uses the airfoil data banks, the numerical routine has used values for angle of attack that correspond to maximum lift to drag ratios at each radial location for each propeller disk.

As previously discussed, there exists a difficulty in the calculation of chord lengths in the region near the hub. In this segment of the blade, the structural requirements force the airfoil to take on the characteristics of a circular cylinder. As a result, the solidity-lift coefficient may take on negative values as the shank region of the propeller is approached because of large values of C_D and relatively small values of C_L. As noted in Eq. (5), for large values of C_D/C_L, the numerator becomes negative. Examination of Eq. (20) indicates that for negative solidity-lift coefficients, the chord length would also result in a negative value. In the present study, it was determined that the most acceptable means to calculate chord length in the vicinity of the hub region would be through a linear interpolation of the chord length from the radial location, where the slope of the planform goes positive to a value of zero at $r/R = 0$.

Once the chord length has been calculated, a new value for the solidity-lift coefficient must be found to complete the calculations for the radial variation of thrust and torque, i.e.,

$$\sigma C_L = (\text{No. Blades})(\text{Chord})C_L/D\pi x \tag{24}$$

By this present approach, any possibility of negative chord lengths in the region of the hub during the numerical design procedure is eliminated.

Once the theoretical model had been fully developed, the design method was applied utilizing the NACA four-digit airfoil family to determine the optimum counter-rotating propeller design with respect to performance.

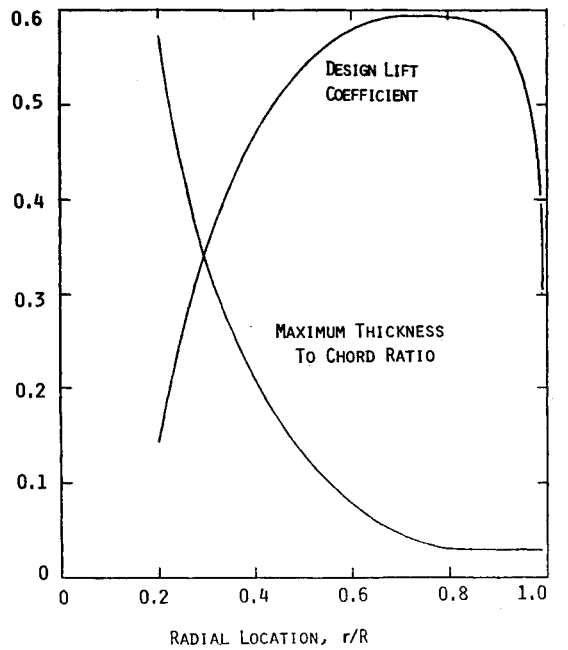

Fig. 4 Assumed values of maximum thickness to chord ratio and design lift coefficient distribution for NACA 4 digit design, both propeller disks.

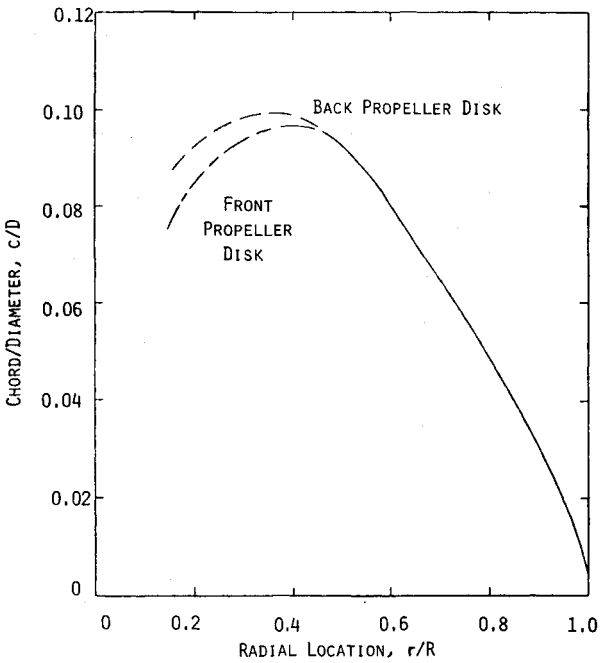

Fig. 5 Resultant chord to diameter distribution using the NACA four-digit airfoil family, front and back propeller disks.

IV. Application of Counter-Rotating Propeller Design Method

Using the NACA four-digit airfoil family, a design for a counter-rotating propeller system was performed. The specified input flight conditions corresponded to a typical commuter class aircraft, i.e., freestream velocity of 625 ft/s, altitude of 28,000 ft, shaft horsepower engine of 900 with the condition that one engine is available for each propeller disk, engine rpm of 1500, and a blade diameter of 7.50 ft. The airfoil maximum thickness to chord distribution, shown in Fig.

4, was dictated by propeller structural considerations. The assumed design lift coefficient radial distribution, shown in Fig. 4, results in a well accepted integrated design lift coefficient of 0.52.

In a study conducted by Korkan and Playle,[18] it was shown that for similar flight conditions, an efficient counter-rotating propeller configuration consisted of six blades per disk. However, it was also shown that there is a small change in total propeller performance between the four-, five-, and six-blade per disk configurations. Based upon this result, a counter-rotating propeller system of four blades per disk was chosen for the present investigation. The spacing between the disks was assumed to be zero, in addition to identical rpm for each propeller disk.

Utilization of the counter-rotating theoretical design model for the conditions previously mentioned results in the developed blade planforms shown in Fig. 5. It may be noted that there is little difference between the front and back propeller disk beyond the radial location of approximately 40%. Before this point, the back propeller chord becomes larger than the front propeller chord. The maximum chords of both disks result in approximately nine inches, which is considered acceptable. The propeller design blade twist distribution, shown in Fig. 6, indicates a significant difference between the front and back propeller disks. This difference in twist comes directly from the effect of the swirl velocity component from the front propeller disk impinging upon the back propeller disk, with the back propeller disk requiring less twist to maintain the angle of attack corresponding to the maximum lift-to-drag ratio.

The differential thrust distributions for the present design, shown in Fig. 7, indicate that the back propeller disk will result in a higher integrated thrust coefficient than the front propeller disk. For this case, $C_T = 0.458$ as compared to a $C_T = 0.330$, respectively, resulting in a total thrust coefficient of 0.788. It may also be noted that the maximum dC_T/dx does not occur at the same radial location for the front and back propeller disks. For example, the front propeller disk maximum dC_T/dx occurs at approximately the 70% radial location, which is considered optimum, whereas the back propeller disk maximum dC_T/dx occurs further inboard at approximately the 60% radial location. The differential power coefficient distribution, shown in Fig. 8, yields identical distributions for the front and back propeller disks due to the condition of equal horsepower being supplied and absorbed by each propeller disk. The integrated power coefficients, i.e., $C_P = 1.378$ and $C_P = 1.395$ with the difference resulting from the iteration tolerance, yields a total power coefficient of 2.773. With the thrust and power coefficient values defined, the resulting propeller efficiencies may be found for the present design and result in $\eta_F = 0.798$ and $\eta_B = 1.093$, hence, a total propeller efficiency of 0.946. It may be noted that a propeller efficiency greater than 100% was found for the propeller back disk. This is a direct result of the swirl velocity component effect and using the conventional expression for calculating propeller efficiency.

The theoretical model previously described, designs a counter-rotating propeller configuration for a given operating condition and specified geometrical constraints. The analysis of the counter-rotating propeller design in an off-design operating condition is also required to determine the full extent of the performance envelope.

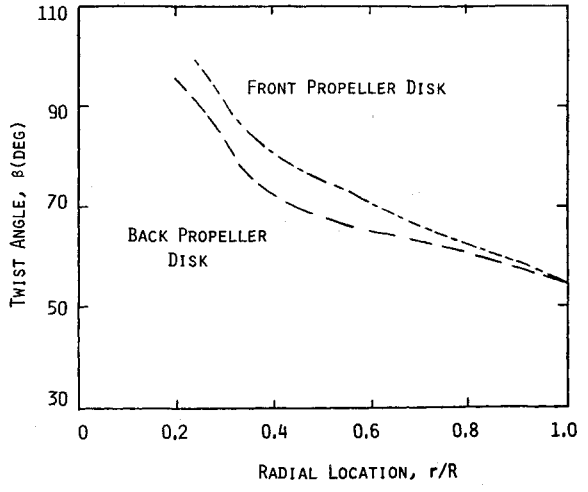

Fig. 6 Resultant propeller blade twist distribution using NACA four-digit airfoil family, front and back propeller disks.

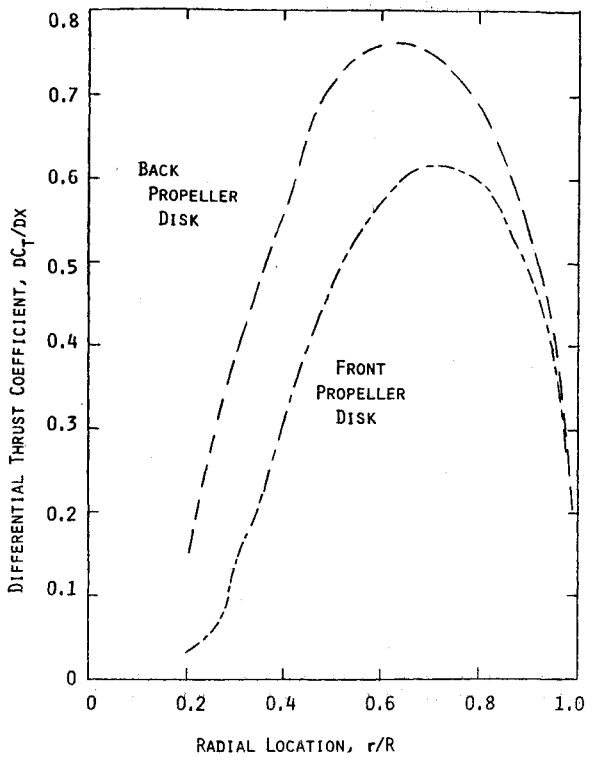

Fig. 7 Resultant differential thrust coefficient distribution using NACA four-digit airfoil family, front and back propeller disks.

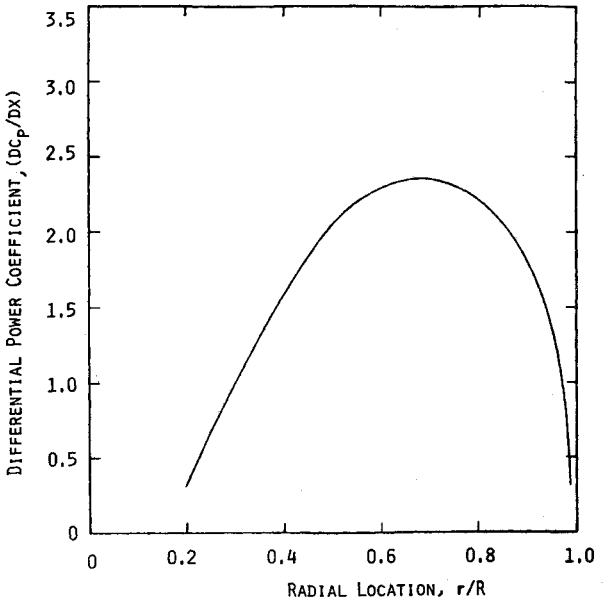

Fig. 8 Resultant differential power coefficient using the NACA four-digit airfoil family, front and back propeller disks.

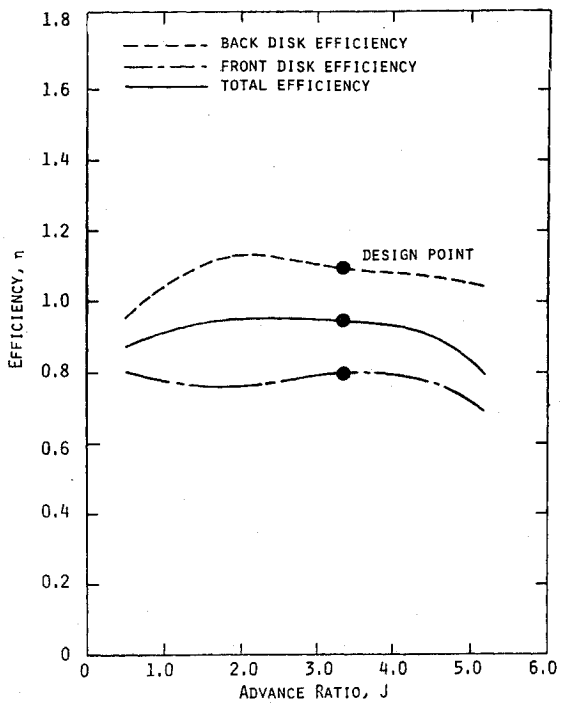

Fig. 9 Off-design efficiency of NACA four-digit counter-rotating propeller configuration.

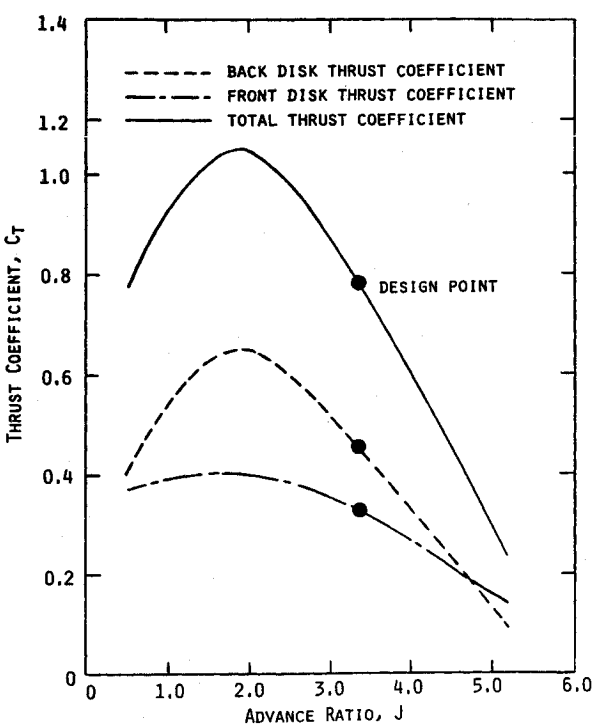

Fig. 10 Off-design thrust coefficient of NACA four-digit counter-rotating propeller configuration.

V. Theoretical Analysis Development

A major reason for the selection of the Lock and Theodorsen design method as given by Davidson, is because of its adaptability to the propeller analysis mode. The analysis method described in the following section uses an iteration scheme to obtain the final results, which converges on airfoil characteristics. To begin the analysis iteration scheme, the propeller blade geometry, such as radial distribution of chord length, twist distribution, and flight condition are specified. The initial value for the airfoil characteristics are also selected, and need only be approximate since the iteration method will

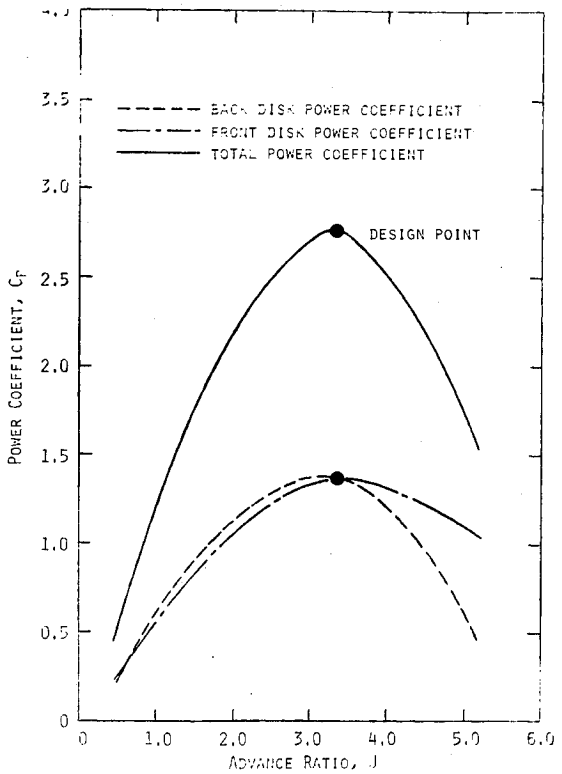

Fig. 11 Off-design power coefficient of NACA four-digit counter-rotating propeller configuration.

result in the actual airfoil data. From these initial airfoil approximations, a value for the solidity may be found,

$$\sigma = (\text{No. Blades})(\text{Chord})/D\pi x \tag{25}$$

Once the value of the solidity has been obtained, values for the interference velocity angles can be computed. Since these angles are functions of the aerodynamics of both propeller disks, the following expressions yield values for B_F and B_B:

$$B_F = (\sigma_F/4X_0\sin\phi_0)(C_{L_F} + X_0 C_{L_B}\cos^2\phi_0) \tag{26}$$

$$B_B = (\sigma_B/4X_0\sin\phi_0)(C_{L_B} + X_0 C_{L_F}(\cos^2\phi_0 - \sin^2\phi_0)) \tag{27}$$

The interference angles define the angle of attack for each radial location since

$$\alpha = \beta - \phi_0 - B \tag{28}$$

These angle-of-attack values yield airfoil characteristics from the airfoil data bank and, therefore, lead to an iteration process by which the final airfoil data used in the performance calculation may be defined. This iteration scheme continues until the airfoil data used at the start of the process results in the interference conditions that yield identical airfoil data.

Once the iteration process has converged, the performance of the counter-rotating propeller is found through the use of Eqs. (8-19) as in the design method. There is no difficulty in calculating values of the circulation function $K(x)$ for the off-design case once the interference values of the velocity are found. Using the above analysis method, a counter-rotating propeller can be analyzed at any given operating flight condition.

VI. Application of Counter-Rotating Propeller Analysis Method

Using the analytical method described in the previous section, an investigation was conducted for the off-design perfor-

mance of the counter-rotating fixed-pitch propeller configuration, designed in Sec. IV, using the NACA four-digit airfoil family. The variation of the advance ratio, J, was obtained by holding the freestream velocity and twist distribution constant and varying the rpm of both the front and back propeller disks, keeping equal values of rpm for both disks.

The resulting values of propeller efficiency are given in Fig. 9 and indicate a very broad and flat efficiency map across a large variance in advance ratio. This result shows that a counter-rotating propeller designed for cruise, will also be efficient in off-design flight conditions such as take-off and climb. Figure 10 indicates a large increase in the thrust coefficient at the lower advance ratios, which is also a definite advantage for the takeoff and climb conditions. The power coefficient decreases at the off-design conditions as given in Fig. 11, but does so in a ratio with the thrust coefficient to yield the relatively flat efficiency curve. These performance calculations have been accomplished at fixed pitch conditions, and it may be assumed that the performance envelope would be further enhanced by utilization of a variable pitch or constant speed mechanism. This series of calculations has indicated the full extent of the advantages of counter-rotating propellers when analyzed in an off-design performance situation. Further, this off-design analysis shows clearly that counter-rotating propellers are not only efficient at the design point, but are also extremely efficient at operating conditions other than the design point.

VII. Conclusions

The theories of Lock and Theodorsen, as described by Davidson, were determined to be acceptable theories for the design and analysis of counter-rotating propellers. Using this theoretical model, the full advantages of counter-rotating propellers have been shown, and indicate approximately, the same efficiency over a large spectrum of operating conditions other than the design point. However, with regards to the limitations of the current model, the radial interference on the front propeller disk is neglected, which is an assumption that may not be totally valid, especially in the hub region. The circulation functions of Theodorsen are calculated for optimum propellers with equal angular velocity on each propeller disk. Although it has been suggested that these values for circulation are still valid for nonoptimum propellers, a question as to their validity for the cases of different angular velocities on each propeller disk may be posed. These cited areas are left for future studies.

Acknowledgment

This research was supported by the National Aeronautics and Space Administration Lewis Research Center, Grant NAG 3-354.

References

[1]Lock, C. N. H., "Interference Velocity for a Close Pair of Contra-Rotating Airscrews, A & M 2084, July 1941.

[2]Biermann, D. and Gray, W. H., "Wind Tunnel Tests of Single- and Dual-Rotating Pusher Propellers Having from 3 to 8 Blades," NACA ARR (WR L-359), February 1942.

[3]Biermann, D. and Hartman, E. P., "Wind Tunnel Tests of Four and Six Blade Single and Dual-Rotating Tractor Propellers," NACA Rept. 747, 1942.

[4]McHugh, J. G. and Pepper, E., "The Characteristics of Two Model 6-Blade Counterrotating Pusher Propellers of Conventional and Improved Aerodynamic Design," NACA ARR (WR L-404), June 1942.

[5]Gray, W. H., "Wind Tunnel Tests of Dual-Rotating Propellers with Systematic Differences in Number of Blades, Blade Setting, and Rotational Speed of Front and Rear Propellers," NACA ARR L4E22 (WR 2-80), May 1944.

[6]Miller, M. F., "Wind Tunnel Vibration Tests of Dual-Rotating Propellers," NACA ARR 3111 (WR L-405), Sept. 1943.

[7]Bartlett, W. A., "Wind-Tunnel Tests of a Dual-Rotating Propeller Having One Component Locked or Windmilling," NACA ARR L5A13a (WR L-214), January 1945.

[8]Strack, W. C., Knip, G., Woesbrich, A. L., Gotston, J., and Bradley, E., "Technology and Benefits of Aircraft Counterrotating Propellers," NASA TM 82983, October 1982.

[9]Ginzel, F., "Calculation of Counterrotating Propellers," NACA TM 1208, March 1949.

[10]*Standard Method of Propeller Performance Estimation,* Society of British Aircrft Constructors, Ltd., London.

[11]Bober, L. J., Private communication, NASA Lewis Research Center, 1983.

[12]Naiman, I., "Method of Calculating Performance of Dual-Rotating Propellers from Airfoil Characteristics," NACA ARR 3E24 (WR L-330), May 1943.

[13]Theodorsen, T., "The Theory of Propellers—Determination of the Circulation and the Mass Coefficient for Dual-Rotating Propellers," NACA Rept. 775, 1944.

[14]Theodorsen, T., *Theory of Propellers,* McGraw-Hill Book Co., New York, 1948.

[15]Davidson, R. E., "Optimization and Performance Calculation of Dual-Rotation Propellers," NASA TP 1948, Dec. 1981.

[16]Playle, S. C., "A Numerical Method for the Design and Analysis of Counter-rotating Propellers," M. Sci. Thesis, Texas A&M Univ., June 1984.

[17]Korkan, K. D., Private communication, Texas A&M Univ., 1984.

[18]Korkan, K. D. and Playle, S. C., "On the Design of Counter-rotating Propellers," SAE Paper 830773, April 1983.